AFRL-RX-WP-TP-2011-4225

HYBRID CONTACT STRESS ANALYSIS OF A TURBINE ENGINE BLADE TO DISK ATTACHMENT (Preprint)

Patrick J. Golden

Metals Branch
Metals, Ceramics & NDE Division

Sam Naboulsi

High Performance Technology, Inc.

JULY 2011

AIR FORCE RESEARCH LABORATORY
MATERIALS AND MANUFACTURING DIRECTORATE
WRIGHT-PATTERSON AIR FORCE BASE, OH 45433-7750
AIR FORCE MATERIEL COMMAND
UNITED STATES AIR FORCE

REPORT DOCUMENTATION PAGE

Form Approved
OMB No. 0704-0188

1. REPORT DATE *(DD-MM-YY)*	2. REPORT TYPE	3. DATES COVERED *(From - To)*
July 2011	Journal Article Preprint	01 July 2011 – 01 July 2011

4. TITLE AND SUBTITLE
HYBRID CONTACT STRESS ANALYSIS OF A TURBINE ENGINE BLADE TO DISK ATTACHMENT (Preprint)

5a. CONTRACT NUMBER
IN-HOUSE

5b. GRANT NUMBER

5c. PROGRAM ELEMENT NUMBER
62102F

6. AUTHOR(S)
Patrick J. Golden (Metals, Ceramics & NDE Division, Metals Branch (AFRL/RXLM))
Sam Naboulsi (High Performance Technology, Inc.)

5d. PROJECT NUMBER
4349

5e. TASK NUMBER
20

5f. WORK UNIT NUMBER
LM110100

7. PERFORMING ORGANIZATION NAME(S) AND ADDRESS(ES)

Metals, Ceramics & NDE Division, Metals Branch (AFRL/RXLM)
Materials and Manufacturing Directorate, Air Force Research Laboratory
Wright-Patterson Air Force Base, OH 45433-7750
Air Force Materiel Command, United States Air Force

High Performance Technology, Inc.

8. PERFORMING ORGANIZATION REPORT NUMBER
AFRL-RX-WP-TP-2011-4225

9. SPONSORING/MONITORING AGENCY NAME(S) AND ADDRESS(ES)

Air Force Research Laboratory
Materials and Manufacturing Directorate
Wright-Patterson Air Force Base, OH 45433-7750
Air Force Materiel Command
United States Air Force

10. SPONSORING/MONITORING AGENCY ACRONYM(S)
AFRL/RXLM

11. SPONSORING/MONITORING AGENCY REPORT NUMBER(S)
AFRL-RX-WP-TP-2011-4225

12. DISTRIBUTION/AVAILABILITY STATEMENT
Approved for public release; distribution unlimited.

13. SUPPLEMENTARY NOTES
PAO case number 88ABW-2010-5380, cleared 06 October 2010. The U.S. Government is joint author of this work and has the right to use, modify, reproduce, release, perform, display, or disclose the work. Submitted to the International Journal of Fatigue.. Document contains color.

14. ABSTRACT
The present investigation examines an analysis methodology for fretting fatigue in a turbine engine fan disk. This is an important problem for the operators of turbine engines, since it is a significant driver of fatigue damage and failure risk of disks. Fretting fatigue in turbine engines occurs when the blade and disk are pressed together in contact and experience a small oscillating relative displacement due to variations in engine speed and vibratory loading. Fretting causes a very high local stress near the edge of contact resulting in wear, nucleation of cracks, and their growth, which can result in significant reduction in the life of the material. It is dependent on geometry, loading conditions, residual stresses, and surface roughness, among other factors. These complexities are not just physically based, but also computationally challenging. For example, the determination of the local contact stresses accurately depends on the mesh resolution of the finite element method (FEM) model. This has been addressed using various approaches.

15. SUBJECT TERMS
fretting fatigue, stress analysis, finite element method, contact stress

16. SECURITY CLASSIFICATION OF:			17. LIMITATION OF ABSTRACT:	18. NUMBER OF PAGES	19a. NAME OF RESPONSIBLE PERSON (Monitor)
a. REPORT	b. ABSTRACT	c. THIS PAGE			Patrick J. Golden
Unclassified	Unclassified	Unclassified	SAR	26	19b. TELEPHONE NUMBER *(Include Area Code)* N/A

Standard Form 298 (Rev. 8-98)
Prescribed by ANSI Std. Z39-18

Hybrid Contact Stress Analysis of a Turbine Engine Blade to Disk Attachment

Patrick J. Golden[1]
Materials and Manufacturing Directorate, Air Force Research Laboratory, Wright-Patterson AFB, OH 45433, USA

Sam Naboulsi
High Performance Technology, Inc., Reston, VA 20190, USA

Abstract

The present investigation examines an analysis methodology for fretting fatigue in a turbine engine fan disk. This is an important problem for the operators of turbine engines, since it is a significant driver of fatigue damage and failure risk of disks. Fretting fatigue in turbine engines occurs when the blade and disk are pressed together in contact and experience a small oscillating relative displacement due to variations in engine speed and vibratory loading. Fretting causes a very high local stress near the edge of contact resulting in wear, nucleation of cracks, and their growth, which can result in significant reduction in the life of the material. It is dependent on geometry, loading conditions, residual stresses, and surface roughness, among other factors. These complexities are not just physically based, but also computationally challenging. For example, the determination of the local contact stresses accurately depends on the mesh resolution of the finite element method (FEM) model. This has been addressed using various approaches. Recently, a computational hybrid technique was implemented successfully to investigate fretting fatigue of turbine engine blade and disk attachments. The present work extends application to specifically investigate the effects of surface contact in an actual blade and disk assembly using a representative loading mission. The results show consistency with available experimental data. Finally, the knowledge gained from this investigation could be used as a basis for uncertainty analyses of an actual blade and disk assembly.

[1] Materials Research Engineer, 2230 Tenth St, Wright-Patterson AFB, OH 45433-7817, USA, Phone: 937-255-5438, FAX: 937-656-4840, E-mail: patrick.golden@wpafb.af.mil

Keywords

Fretting Fatigue, Stress Analysis, Finite Element Method, Contact Stress

1. Introduction

Recently the failure of engines on four jet aircraft overseas during the past two years has prompted the National Transportation Safety Board (NTSB) to issue an "urgent" recommendation to increase inspections of the engines on U.S. aircraft. None of the incidents resulted in crashes, injuries, or fatalities, but in all four cases engine parts penetrated the engine housing. Such uncontained engine failures are particularly dangerous because flying engine parts could puncture fuel or hydraulic lines, damage flight surfaces or even penetrate the fuselage and injure passengers. At issue are older engines found on a small number of jets. The Federal Aviation Administration (FAA) is aware of the problem and issued a rule in March 2010 requiring inspections of the engines within 50 flights, and repeat inspections every 175 flights thereafter. The NTSB issued its urgent recommendation, saying the FAA should require inspections every 15 flights until the disks can be replaced with improved parts. It also prompted the FAA to work on a rule that would add testing of the rotor disks for cracks. These actions show the safety and economic impact fatigue damage and fracture risk can have on aircraft engines. To be more specific, fretting, which is one of the primary phenomena that leads to damage or failure of blade-disk attachments, is of interest and the focus of the present paper.

The focus of the current work is on damage tolerance and risk calculation of rotating turbine engine disks with fretting induced damage. Prior work has shown that the very high edge-of-contact stresses coupled with fretting induced surface damage can lead to early fatigue crack formation and accelerated crack propagation [1-3]. Previous research has shown that with accurate stress calculations and the use of appropriate weight function stress intensity factor

solutions, the influence of the contact stress field on crack propagation can be predicted [4-7]. Likewise, the presence of coatings or surface residual stress treatments has also been shown to influence the rate of crack propagation in fretting fatigue in a predictable way [8].

Operators of turbine engines, particularly in the United States military, continue to look for ways to increase safety, reliability, and reduce sustainment costs. Probabilistic damage tolerance analysis is one approach to enable these goals through the quantification of the effect of usage strategies, inspections, and fatigue damage mitigation techniques on the risk or probability of fracture. A software tool has been developed through FAA funding to implement probabilistic damage tolerance assessment of turbine engine disks with internal or surface anomaly distributions [9]. Increased use of this and other tools for probabilistic assessment of fracture critical components is currently being pursued by designers and operators of turbine engines.

The objective of the current work is to develop an efficient yet accurate method of stress analysis for a three-dimensional (3-D) engine disk in the blade attachment region where fretting occurs. The stress gradients are needed to feed a probabilistic fracture prediction of the disk due to fretting cracks and ultimately to be able to assess the influence of fretting mitigation strategies such as coatings, inspections, and surface residual stress treatments on the probability of failure. The approach was to combine a finite element method (FEM) model of the full 3-D geometry with a 2-D numerical contact stress analysis tool. The paper will describe this approach in detail and demonstrate it through analysis of a fan blade to disk attachment region of a military turbine engine with a realistic engine speed mission. Verification of several steps of the approach including a simple mesh refinement study was conducted.

2. Methodology

Fretting fatigue can occur in a gas turbine engine when the blade and disk are pressed together in contact and experience a small oscillating displacement. It is a complex phenomenon that depends on geometry, loading conditions, residual stresses, and surface roughness, among other factors. These complexities also go beyond the physics of material interactions and into the computational domain. For example, accurate determination of the local contact stresses depends on the FEM mesh resolution. These computational issues are further magnified when dealing with models that resemble a geometrically complex real life problem. Hence, an approximate approach is needed to keep the problem computationally feasible, which is the case in this study. A Computationally Hybrid Technique (CHT) will be presented to study the life prediction of a blade-disk assembly, which is versatile in complex practical problems considering both contact and fracture mechanics. The CHT method is based on the use of the FEM technique to compute the integrated contact forces on the fretting surfaces, followed by the solutions to a set of Singular-Integral-Equations (SIE) to compute the local contact stresses accurately. The reason of combining the FEM and the SIE approach is that each has an advantage and a disadvantage in terms of accuracy and efficiency. The FEM solution accounts for all of the component geometric features, whereas the SIE solution does not. The SIE solution is fast and accurate at obtaining the local contact stress, whereas the FEM contact solution has a long computational time, and reaching a converged stress solution at the edge of contact is ambiguous, especially in 3-D models. The CHT takes advantage of both the FEM and SIE strengths by computing the total stresses through the combination of the computed FEM bulk stresses (i.e. eliminating contact stress influence) and the SIE contact stresses. It encompasses computational versatility and accuracy for geometrically complex components in contact.

Further, the CHT method provides a tool to calculate crack nucleation and crack growth through fracture mechanics stress intensity factor, K. Nucleation is computed any number of stress and strain based multiaxial fatigue approaches. Stress intensity factors are calculated based on the weight function methodology, and it allows for stress ratio, R, values to account for residual stress or compressive applied loading. In this case, superposition of the residual stress mode I stress intensity factor, K_I, with the maximum and minimum applied K_I resulted in a total maximum and minimum K_I. Then effective stress intensity factor range, ΔK_{eff}, that accounts for the changing R, can be calculated [8]. The present fretting work uses the available Mode I surface crack and through crack weight function K solutions [10]. This is consistent with previous work [11], which has shown that any mode II contribution to crack growth was expected to be quite small.

Next, the computational methodology behind the CHT will be presented. First, a finite element analysis of the blade and disk assembly is performed. The model is nonlinear due to contact at the two blade to disk interfaces. Once results are obtained, the FEM contact surface is divided into a finite number of slices by the CHT as shown in Figure 1, which allows one to compute the contact force histories at each slice. Figure 1 is an cutaway drawing of the disk slot with the blade removed. The 12 slices were made perpendicular to the contact plane and equally spaced along the axial length of the slot in this case. The FEM analysis includes both the applied inertial load and the statically applied steady-state aerodynamic forces on the airfoil. Figure 2 is a plot of an example set of the pressure, $p(x)$, and shear, $q(x)$, contact tractions extracted from the FEM results at one point in the load history and at one slice.

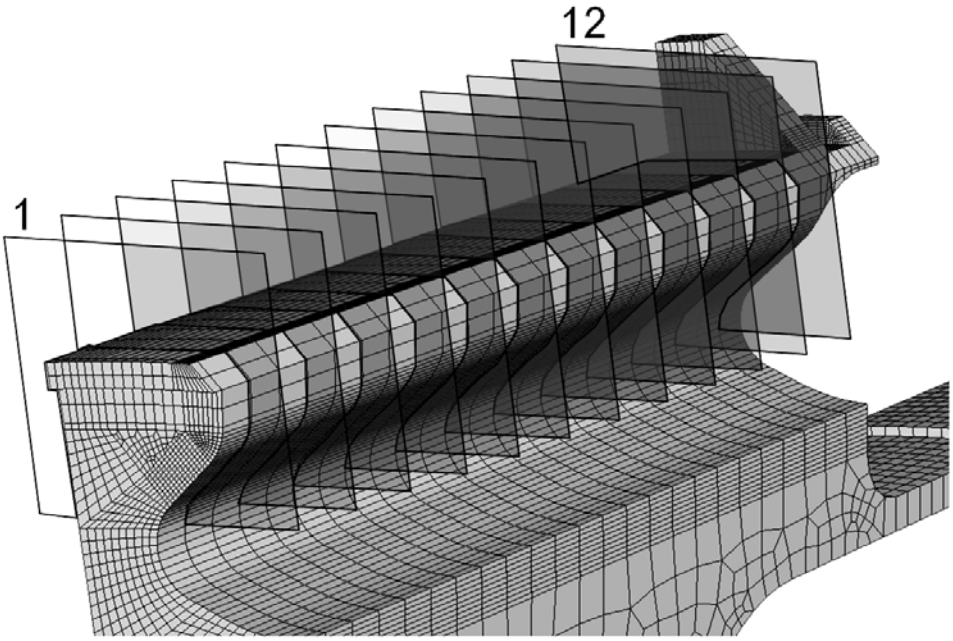

Figure 1: Schematic drawing of the location of 2-D slices overlaid on the disk blade slot mesh. The mesh shown is a cut away drawing of half the disk sector with the blade removed.

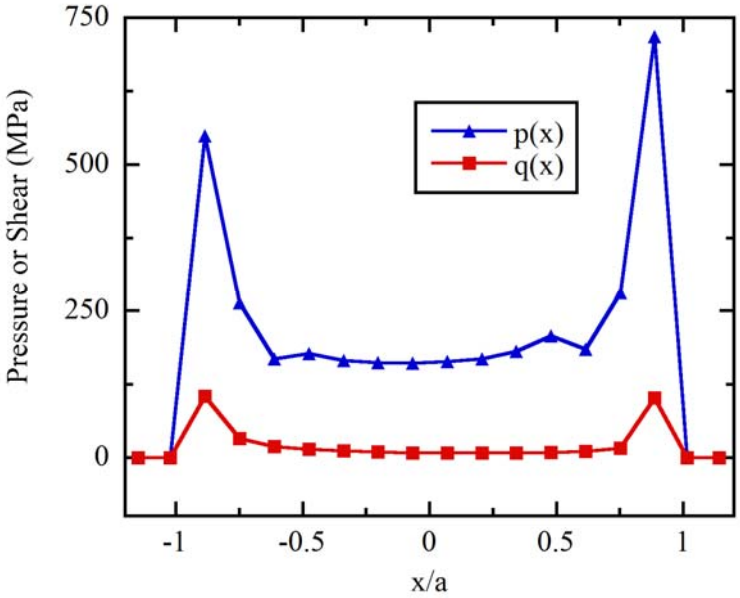

Figure 2: Example FEM pressure and shear tractions at one slice and one engine speed.

Second, the contact forces are computed from the tractions at each slice. The tractions are integrated on the two-dimensional (2-D) plane leading to calculation of the normal contact force per unit thickness, P, the shear contact force per unit thickness Q, and the contact moment

per unit thickness M about the center of contact associated with fretting. These were obtained by integrating the contact pressure p over the contact length x, the shear traction q over the contact length x, and the product of the contact pressure p and the distance from the center of contact, x_0, respectively as shown in Equations 1-3.

$$P = \int p(x)dx \tag{1}$$

$$Q = \int q(x)dx \tag{2}$$

$$M = \int (x - x_0)p(x)dx \tag{3}$$

The relationship among contact forces P and Q at a single slice is illustrated in Figure 3.a) for a simple fan speed profile. The dashed lines indicate the bounds imposed by the coefficient of friction μ and described by equation 4. Note that the contact forces P and Q are related for a typical fan speed profile by either gross slip (i.e. sliding) which occurs when $|Q| = \mu P$ or partial slip which occurs when $|Q| < \mu P$.

$$|Q| \leq \mu P \tag{4}$$

Note that a characteristic value of the Q versus P slope (dQ/dP) exists during partial slip, and it depends on the model's geometry and stiffness. Also, the coefficient of friction can vary during the cyclic life based on experimental observation. Experiments in Golden [12] showed that despite the changing value of μ over the life of the experiment the characteristic value of dQ/dP did not change. Figure 3.b) shows the history of the calculated moment arm, δ, for the same slice where δ is defined by Equation 5. The conclusion from analysis of all slices is that this value remains relatively small and constant and was treated as a constant value for each slice.

$$M = \delta P \tag{5}$$

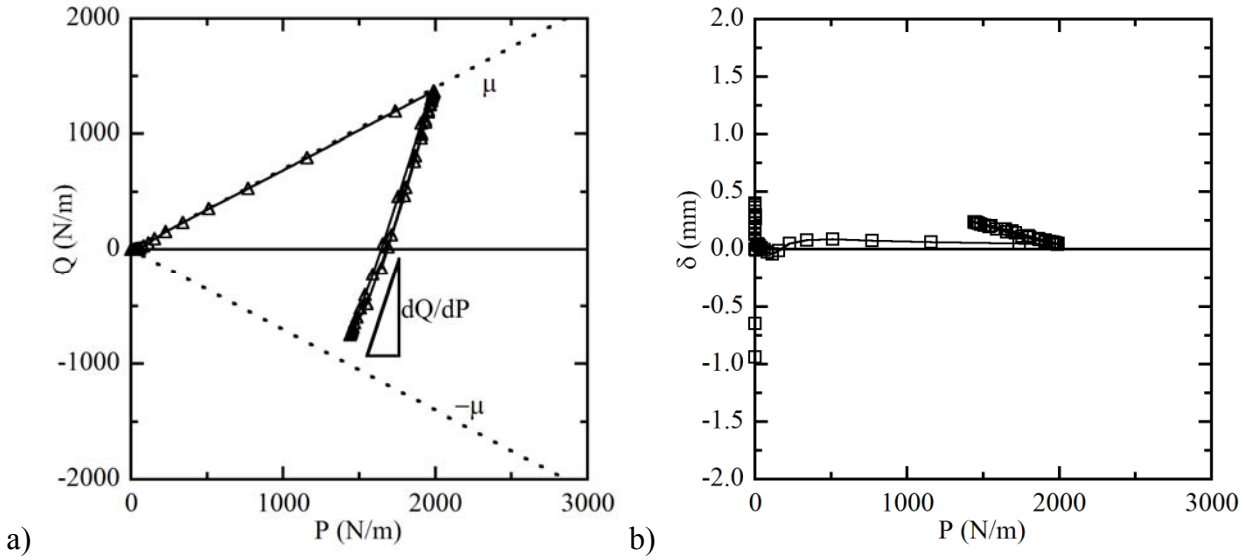

Figure 3: Contact load histories integrated from finite element tractions for one zone showing a) Q versus P and b) δ versus P. The definition of the partial slip slope, dQ/dP, is shown in a).

Third, the computed contact forces at each slice are used to compute the contact stresses accurately utilizing the SIE based CAPRI software [13,14]. It is a SIE solver, which computes the contact stresses for a random shaped indenter pressing into a flat plate. The indenter shape is chosen to be an equivalent geometry as that of the real component which is typically flat with rounded edges. The normal force, P; shear force, Q; and moment, M, as shown in Figure 3, are applied using a Fast Fourier Transform (FFT) technique. The distributions of normal traction, $p(x)$, and shear traction, $q(x)$, on the fretting surfaces are computed using the singular-integral-equations formulation as demonstrated for a flat with rounded edge contact problem by Ciavarella et al. [15]. Series expansions are then performed for $p(x)$ and $q(x)$ in terms of Chebyshev's polynomials, which are then utilized to obtain the Mushkelishivili potential. The interior stress field is evaluated from Mushkelishivili's potential using standard equations.

Fourth, the bulk stresses at each slice along a variable path (i.e. normal to the contact surface or at a prescribed angle θ) for a prescribed depth, which is shown in Figure 5, is

computed from the FEM analysis. The bulk stress is the total stress minus the contribution of the local contact stress at a given point. It captures the tension and bending stress fields in the disk that cannot be determined with the SIE solution. It is computed by extracting the multi-axial components of the FEM stress along a path pointing outward to the contact interface and starting at the edge of contact. Figure 6 shows the FEM stresses at a given slice where x is parallel to the contact surface in the plane of the slice, y is in the direction of the path, and z is out of the plane in the axial direction of the slot. Note that σ_{xx} shows the additive effect of the local contact stress gradient as the path approaches the edge of contact. Hence, by extrapolating the linear stress gradient away from the surface, the bulk stress, σ_{bulk}, is approximated as shown by the dashed line in Figure 6. Note that the other multi-axial components of stress are relatively small and can be ignored in the present work.

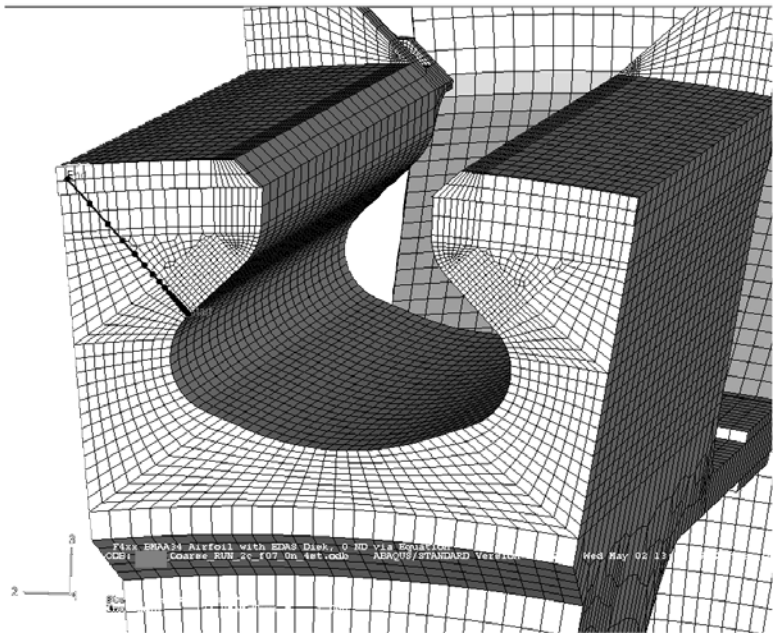

Figure 5: Mesh of the dovetail slot showing the type of path used to extract the subsurface stress gradient used for bulk stress calculation.

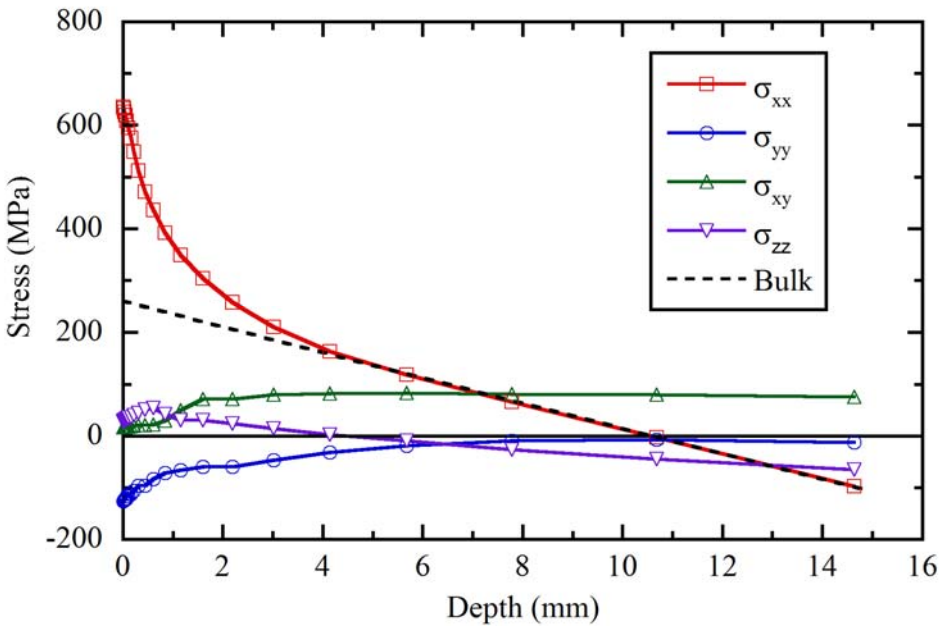

Figure 6: Plot of the multiaxial stress components extracted from the coarse FEM model starting on the surface at the edge of contact. The bulk stress is approximated by a linear gradient extrapolated from the subsurface σ_{xx} results, ignoring the near surface contact effects.

Finally, the total fretting fatigue stresses are computed by adding the SIE contact stresses and the FEM bulk stresses for each mission point and each slice. The total fretting stresses are then utilized to compute the stress intensity factors and fatigue crack growth rate response using the weight function methodology as has been described in prior work [7,16].

3. Modeling, Analysis, and Results

In this section, the capabilities of the CHT will be demonstrated. The focus will be on the sensitivities of the results to the finite element model. Three areas will be investigated, which are loading, friction at the contact surface, and mesh refinement. The finite element meshes used in this investigation will be presented first.

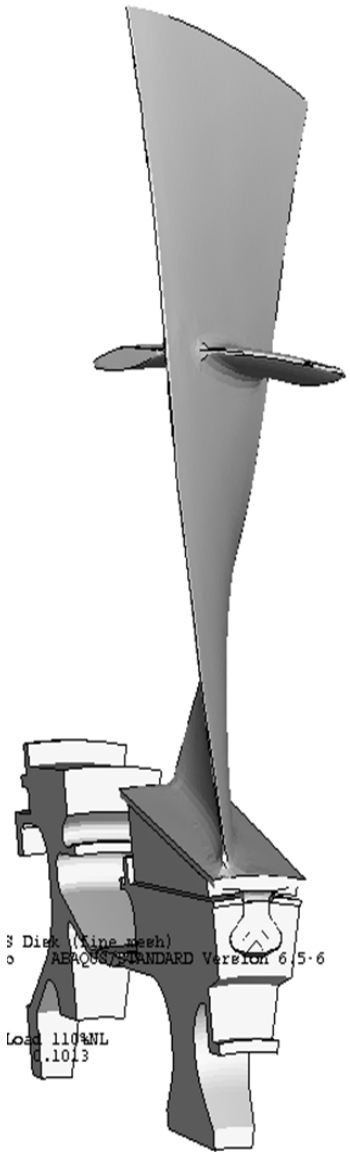

Figure 7: Solid model representation of the blade/disk geometry modeled in this work.

The finite element mesh models a nominal geometry of a turbine engine's fan blade in contact with a disk. The nominal blade geometry includes a snubber. The geometry is shown in Figure 7. The finite element model meshes a single blade in contact with a section of a disk. However, the effects of a single stage rotor disk (i.e. the full 360 degrees) are included by using cyclic symmetry boundary conditions for the disk and snubber sections. The cyclic symmetry conditions assume that all blades are geometrically identical and have an identical response. The

finite element meshes use various elements, which are linear hexahedral elements, linear wedge elements, and linear tetrahedral elements. Two meshes are used in the present study to investigate the mesh sensitivity on the CHT's results, which are a coarse mesh and a fine mesh. The main difference is the element sizes and density near the dovetail region and contact surfaces. A comparison is shown in Figure 8. The total numbers of degree of freedoms for the fine and coarse meshes are 2,189,382 and 362,712, respectively. The contact surface for the coarse mesh has arrays of 24 equal size elements along the depth of the dovetail slot. But, the fine mesh has 89 elements along the depth of the dovetail slot with a bias distribution that has higher density at the leading and trailing edges. In the radial direction of the dovetail slot the disk fin and coarse meshes have approximately 32 and 16 elements in contact, respectively. The ABAQUS software is used to perform the analyses and the contact surface is modeled using a surface-to-surface contact formulation. Static analyses are used where the inertia loading is applied first to model the spinning of the rotor. Then, a nominal load distribution along the blade's suction and pressure sides are applied statically to model an aerodynamic loading scenario.

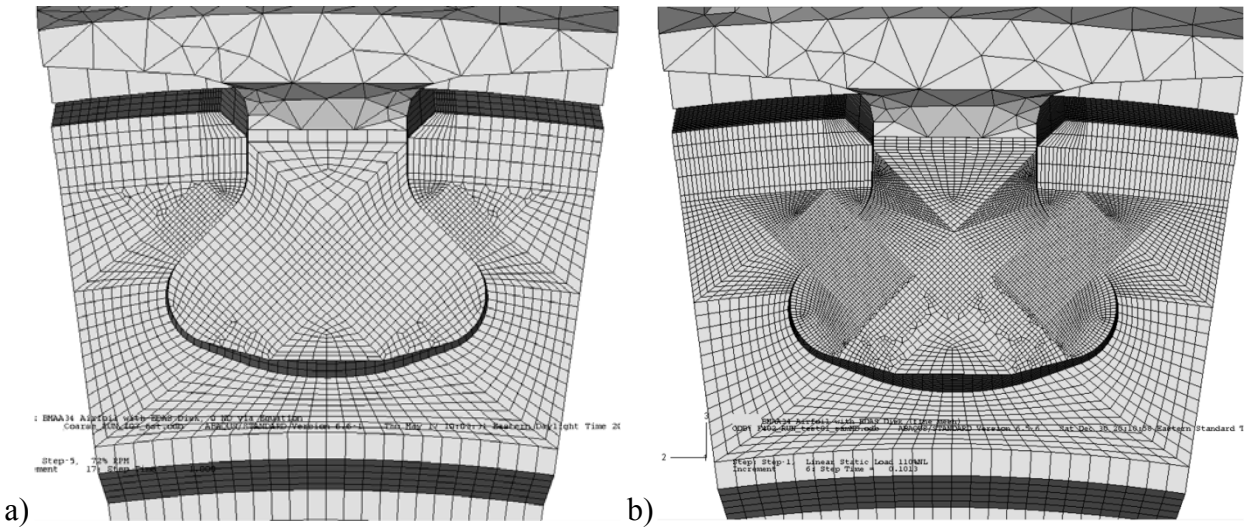

a) b)

Figure 8: Mesh of a portion of the disk containing one blade slot and the blade dovetail region including the blade platform at the top of the image. Both the a) coarse and b) fine meshes are shown. The disk radial direction is vertical and the axial flow direction is into the page.

Turbine engine components experience variable amplitude loading histories, which may consist of periodic overloads, overload or underload combinations, and periods of sustained load interspersed among relatively constant amplitude loading. This results in high operating stresses and severe service environments. In the present study two loading spectrum cases are used. The first is a nominal loading spectrum that is representative of the complex varieties of in-service variable amplitude loading histories. The loading spectrum consists of 34 engine speed reversals varying between 105% and 26% of maximum fan speed. This nominal load spectrum is computationally expensive in FEM analyses. The second load spectrum is a simplified one. It consists of 4 reversals, which are 110%, 50%, 110%, and 72% of maximum fan speed. It is computationally efficient compared to the nominal loading spectrum. It was therefore desired, under the CHT, to model only the simplified load spectrum. Then those results could be used with the method described previously to predict the contact force and bulk stress history for any complex fan speed mission. Figure 8 is a plot of a predicted Q versus P history for the nominal loading spectrum of 34 reversals. The predicted values of Q and P are shown as points with the

dashed line, while the solid line are the results from the purely FEM analysis of the model for the full nominal mission. The comparison shows that the predicted results are slightly different from the full FEM results. For this particular slice, the FEM analysis results in higher peak contact forces. An analysis of all slices shows that there can be some redistribution of the contact pressure and shear tractions along the axial length of the dovetail slot which cannot be predicted using the CHT. Considering that the predicted load history takes seconds to compute and the FEM results can take many hours or even days for some spectra, the difference in contact forces is small.

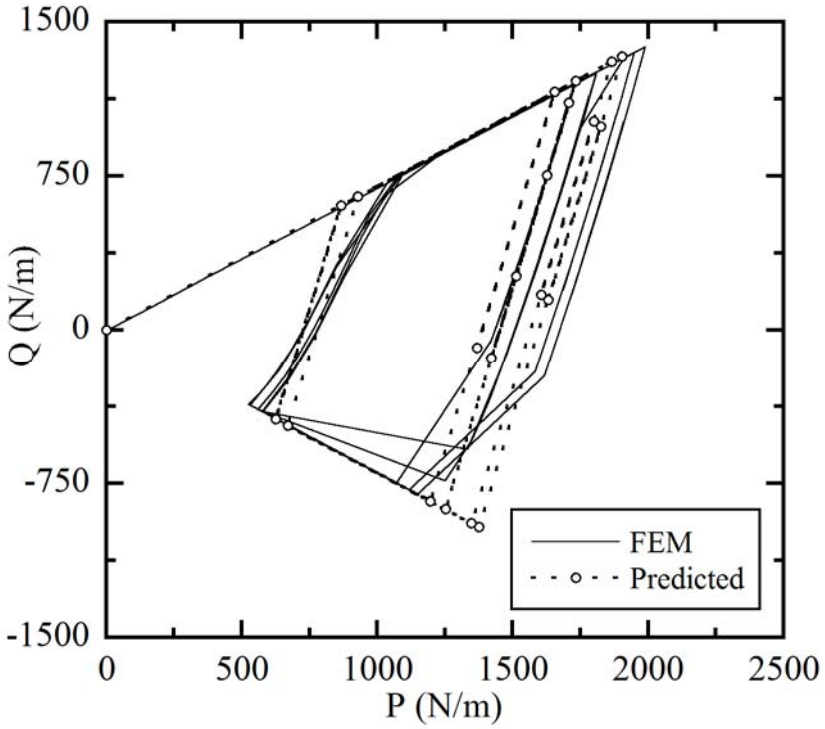

Figure 8: Comparison of mission contact force history as calculated from a full mission FEM analysis and as predicted based on the results of a simple mission FEM analysis.

A parametric study of variable coefficient of friction was performed to investigate the sensitivity of the contact forces to the friction coefficients. Three coefficients of friction are used at the contact surface employing the nominal loading spectrum, which are 0.5, 0.7, and 0.9.

They are compared to the 0.7 coefficient of friction case employing the simplified loading spectrum. The coarse mesh is used for all of these cases. The results for the normal versus the tangential contact forces are plotted in Figure 9 for one representative slice. The results show the following. The tangential contact force's magnitudes increased with higher coefficient of friction as expected. This varied among slices along the axial length of the slot. The contact forces Q versus P for the nominal loading spectrum continued to exhibit a wide gross slip hysteresis loop for all coefficients of friction due to the very low minimum fan speed in the nominal mission that forces the blade to slide within the disk slot. However, the hysteresis loop widened as the coefficient of friction was reduced. This indicates larger gross slip influence at lower coefficient of friction. The contact forces Q versus P slope (dQ/dP) varied only slightly with different coefficients of frictions, however, the variation of the partial slip dQ/dP from slice to slice was much greater than the variation at a single slice due to the influence of μ. The small variation in partial slip dQ/dP with μ and with time is consistent with the experimental results shown in Golden [16].

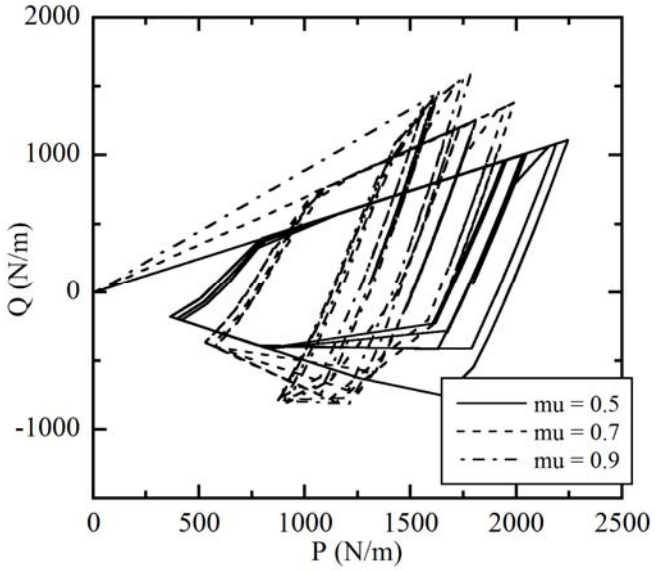

Figure 9: FEM contact load history results for a full mission at one slice showing the influence of coefficient of friction on the gross slip and partial slip behavior of the contact.

Mesh sensitivities were also investigated. The contact surface of the coarse mesh had 12 slices along the depth of the dovetail slot. But, the refined mesh has 89 slices. Figure 10 shows a comparison of the two meshes in the dovetail region. The simplified loading spectrum and μ of 0.7 is used for both analyses. The pressure and shear tractions along both contact surfaces (i.e. Hi and Lo) for both coarse and fine meshes were plotted for the 110% loading point in Figure 10. The results show a considerable difference in the contact stresses at the leading and trailing edges between the coarse and refined mesh as expected, since the contact stresses were sensitive to the mesh size in the vicinity of the contact surface. The contact forces were also plotted for the first slice as a function of the normalized blade force due to the inertia loading. The results are shown in Figure 11 for the normal and shear forces. The results show less sensitivity of the contact forces to the mesh than the contact stresses. Based on the results of the two meshes, the contact forces and the bulk stresses show sensitivities to the mesh refinement. The extent of such sensitivity requires a full convergence study, which is very time consuming and beyond the scope of this investigation. But, considering the versatility of the CTH and the replacement of the less accurate FEM contact stresses with a more accurate SIE one, the trade off of using the coarse mesh are well justified. Especially, that the refined mesh or an ultimate refined mesh, that might results from a convergence study, is computationally expensive and impractical for the problem of interest.

a)

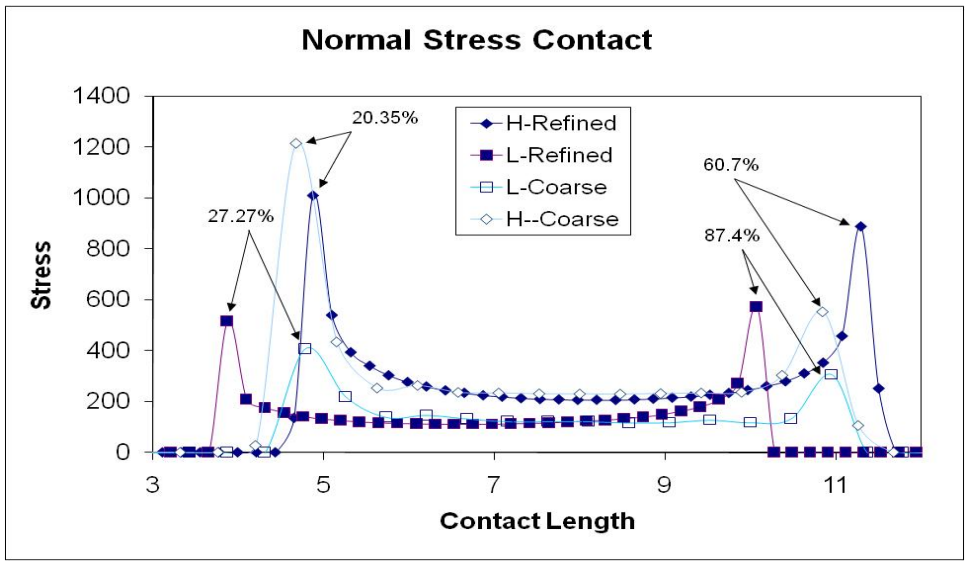

b)

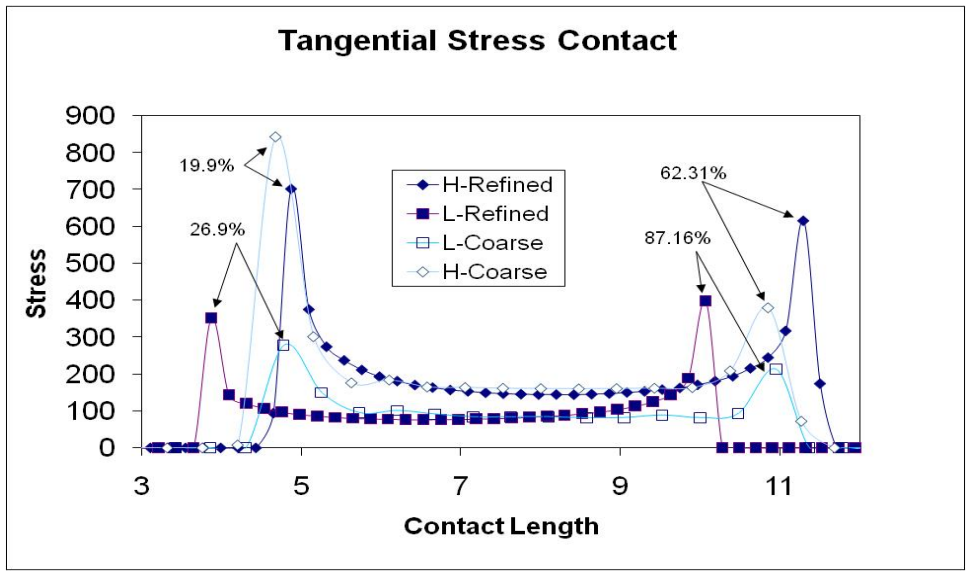

Figure 10: Comparison of the fine and coarse mesh contact tractions at one point in time and for one slice showing a significant difference in peak a) pressure and b) shear tractions.

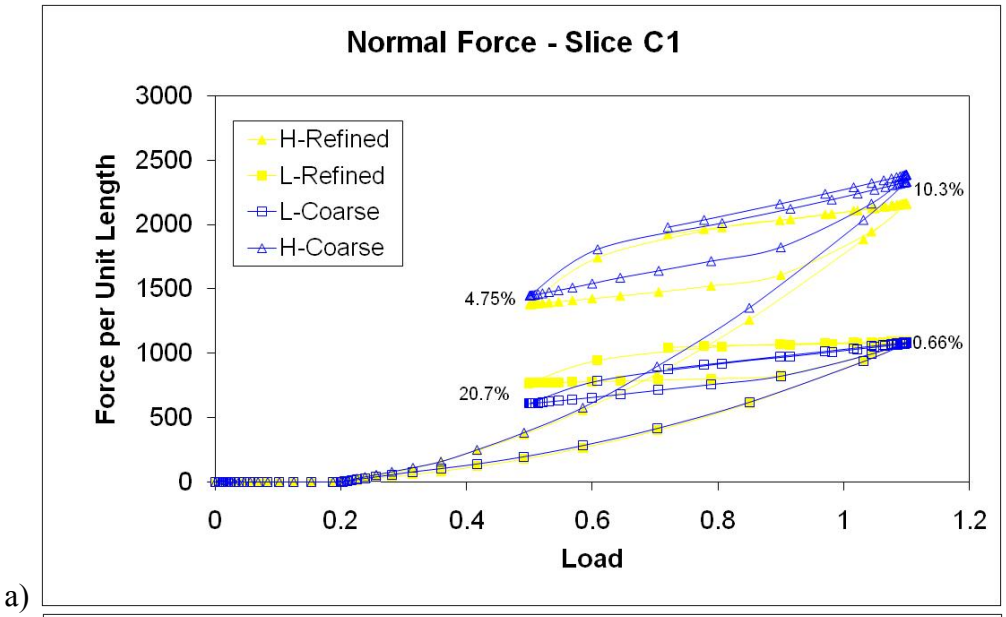

a)

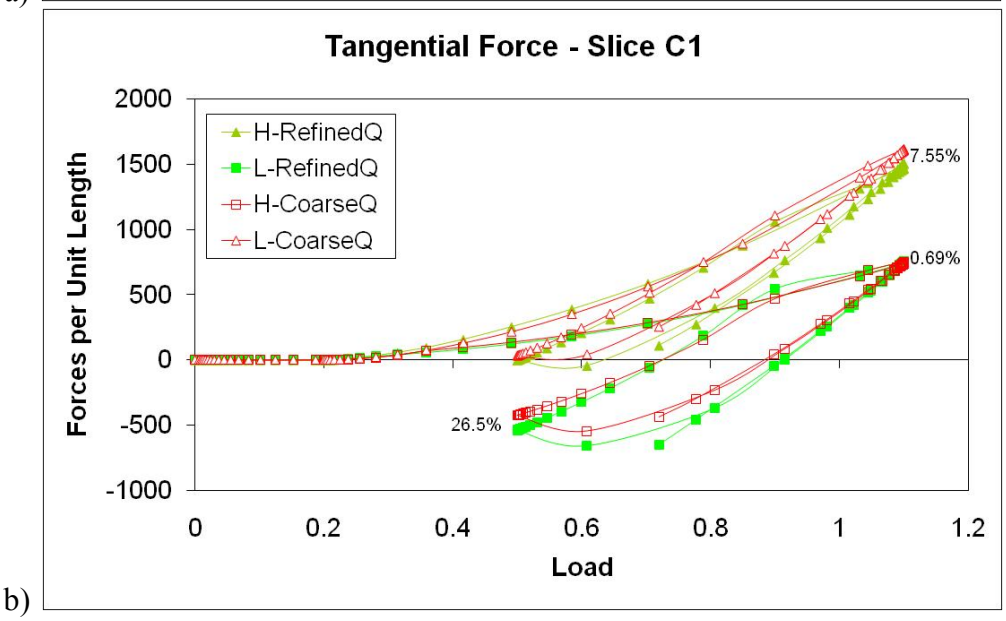

b)

Figure 11: Comparison of the fine and coarse mesh contact force time histories for two different slices showing a lesser difference in integrated forces compared to peak stresses.

6. Conclusions

Several conclusions can be made from this work. The computational hybrid technique (CHT) has been shown to be an efficient and accurate approach to obtain the necessary stress distributions needed to perform a damage tolerance analysis of a blade to disk fretting problem. The combination of a coarse 3-D FEM model of the components with a numerical solution to the

2-D singular integral equations for contact yields a full stress distribution at the edge of contact where cracks have been shown to form and grow. Dividing the 3-D problem into multiple 2-D slices for analysis was shown to dramatically speed up computation times with little loss of accuracy. Very fast contact force history predictions in the dovetail slot for complex loading spectra were demonstrated and shown to be reasonably accurate without the need for additional FEM analyses. A simple mesh refinement study showed that a more refined 3-D FEM mesh resulted in very little benefit over the more coarse mesh. Finally, a parametric study for the effect of coefficient of friction confirmed the importance of this parameter on the predicted stress results.

Acknowledgements

This work was partially supported by the Naval Air Systems Command under agreement EDO-08-SA-0021, and Dr. Ramesh Chandra, NAVAIR, is the technical point of contact for this activity. The technical collaboration with Dr. Michael Enright and Dr. Kwai Chan is also acknowledged.

References

[1] Nicholas T. Critical Issues in High Cycle Fatigue. Int J Fatigue 1999;21:S221-31.

[2] Waterhouse RB. Avoidance of Fretting Fatigue. In: Waterhouse RB, editor. Fretting fatigue. London: Applied Science Publishers Ltd.; 1981. p. 221-40.

[3] Szolwinski MP, Farris TN. Mechanics of Fretting Fatigue Crack Formation. Wear 1996;198:93-107.

[4] Rooke DP, Jones, DA. Stress Intensity Factors in Fretting Fatigue. J Strain Analysis 1979;14:1-6.

[5] Hattori T, Nakamura M, Sakata H, Watanabe T. Fretting Fatigue Analysis Using Fracture Mechanics. JSME Int J 1988;31:100-107.

[6] Chan KS, Lee Y, Davidson DL, Hudak SJ Jr. A Fracture Mechanics Approach to High Cycle Fretting Fatigue Based on the Worst Case Fret Concept – I. Model Development. Int J Fracture 2001;112:299-330.

[7] Golden PJ, Grandt Jr AF. Fracture Mechanics Based Fretting Fatigue Life Predictions in Ti–6Al–4V. Eng Fract Mech 2004;71:2229–43.

[8] Golden PJ, Shepard MJ. Life Prediction of Fretting Fatigue with Advanced Surface Treatments. Mat Sci Eng A 2007; 468-470;15-22.

[9] Wu YT, Enright MP, Millwater HR, Probabilistic Methods for Design Assessment of Reliability with Inspection. AIAA Journal 2002;40:937-46.

[10] Shen G, Glinka G. Weight Functions for a Surface Semi-elliptical Crack in a Finite Thickness Plate. Theory Appl Fract Mech 1991;15:247–55.

[11] Nicholas T, Hutson A, John R, Olson S. A Fracture Mechanics Methodology Assessment for Fretting Fatigue. Int J Fatigue 2003;25:1069–77.

[12] Golden PJ. Development of a Dovetail Fretting Fatigue Fixture for Turbine Engine Materials. Int J Fatigue 2009;31:620-28.

[13] McVeigh PA, Harish G, Farris TN, Szolwinski MP. Modeling Interfacial Conditions in Nominally Flat Contacts for Application to Fretting Fatigue of Turbine Engine Components. Int J Fatigue 1999;21:S157–65.

[14] Murthy H, Harish G, Farris TN. Efficient Modeling of Fretting of Blade/Disk Contacts Including Load History Effects. J Tribol 2004;126:56–64.

[15] Ciavarella M, Hills DA, Monno G, The Influence of Rounded Edges on Indentation by a Flat Punch. Proc Inst Mech Eng 1998;212(Part C):319–28.

[16] Golden PJ, Calcaterra JR. A Fracture Mechanics Life Prediction Methodology Applied to Dovetail Fretting. Tribol Int 2006;39:1172–1180.